

P.S.

Donders Graduate School for Cognitive Neuroscience
Master of Science Programme
MSc Thesis

Concept Representations in the Medial Temporal Lobe:
A high-field fMRI study
by
Lonja Simon Schürmann

Supervised by:

1. Sander Bosch
2. Dr. Christian F. Doeller

Radboud University Nijmegen

August 11, 2014

Lonja Simon Schürmann
Student number: 3004074

“It’s bilateral, therefore it must mean something.”

- Sander Bosch

Contents

| | |
|---|----|
| Abstract | 4 |
| Introduction | 5 |
| Methods | 8 |
| <i>Participants</i> | 8 |
| <i>Stimuli</i> | 8 |
| <i>Experimental design</i> | 9 |
| <i>FMRI data acquisition</i> | 10 |
| <i>Behavioral data analysis</i> | 10 |
| <i>FMRI data preprocessing</i> | 10 |
| <i>Analysis of fMRI time series</i> | 11 |
| <i>Representational Similarity Analysis</i> | 12 |
| Results | 14 |
| <i>Behavioral results</i> | 14 |
| <i>Familiarity</i> | 14 |
| <i>Reaction time</i> | 14 |
| <i>Accuracy</i> | 15 |
| <i>Arena task</i> | 15 |
| <i>Imaging results</i> | 17 |
| <i>Category representation</i> | 19 |
| <i>Concept representation</i> | 21 |
| Discussion | 22 |
| References | 27 |
| Supplementary material | 34 |
| <i>Experimental stimuli</i> | 36 |
| <i>Arena task</i> | 36 |
| <i>Imaging results</i> | 37 |

Abstract

Conceptual knowledge has been suggested to be represented in sparse networks of ‘concept cells’ in the medial temporal lobe (MTL), following the discovery of cells that selectively fire in response to a single concept in a modality-invariant manner, e.g. different pictures of Jennifer Aniston. Here we aim to probe these distributed small-scale ensembles of concept representations using high-field fMRI at 7-Tesla and Representational Similarity Analysis. Subjects viewed pictures of four categories (faces, animals, objects & scenes) belonging to one of two superordinate concepts (the fantasy worlds of *Harry Potter* and *Lord of the Rings*). We tested representational content on both the categorical and the conceptual level using univariate and multivariate methods. We found evidence for distributed category representations along the ventral visual stream and limited evidence for an involvement of the perirhinal cortex in the representation of conceptual knowledge.

Introduction

Since the fifties of the last century, memory theories have identified the hippocampus as a key structure in supporting the formation of unique episodic memories (Scoville & Milner, 1957; Eichenbaum et al., 1999). However, in recent years, evidence for a more integrative function of the hippocampus has emerged (Shohamy & Wagner, 2008; Staresina & Davachi, 2009). In this view, the hippocampus is not solely involved in encoding unique experiences, but also in supporting their dynamic integration into an associative network that extends beyond individual events. It has been suggested that the hippocampus subserves this function by abstracting commonalities shared across multiple related experiences (Kumaran et al., 2009, 2012; Milivojevic & Doeller, 2013).

The human conceptual system arguably relies on the abstraction of meaning to form and represent semantic knowledge about the world, ‘concepts’, efficiently (Barsalou et al., 2003). This puts the hippocampus at the heart of conceptual learning processes. Evidence for conceptual representations in the hippocampus was indeed found in a single-cell recording study in humans (Quian Quiroga, 2005). In this study, epileptic patients implanted with intracranial electrodes were shown pictures of famous people, animals, objects or scenes. Cells were found that selectively fired in response to a single visual stimulus, maintaining their invariant representation across different pictures of the same object and even different modalities (visual, spoken and written, Quian Quiroga, 2009). For example, one hippocampal neuron showed selective firing to seven different pictures of Jennifer Aniston, but not to eighty other pictures. This led to the conclusion that these neurons, named ‘concept cells’, might be the pinnacle of the abstraction process needed to encode a conceptual representation characterized by invariance to the low-level features of the image. From the very selective firing of MTL neurons it was possible to infer which concept was shown to the subject with a success rate above chance, demonstrating the explicit content of MTL neurons compared to early visual areas, which do not distinguish between pictures of the same person and of different persons. Though difficult to define (Putnam, 1973; Fodor, 1998; Millikan, 1998), here we adhere to the operational definition of a concept that was used in Quian Quiroga (2005), i.e. ‘an abstract representation that is invariant to the metric characteristics of the percept’.

How might a finite number of concept cells represent the thousands of concepts we typically remember? It has been argued that MTL neurons might be organized in sparse networks, each representing one concept (Quian Quiroga, 2012). This idea is in line with the high, yet not

quite perfect, selectivity of MTL neuron firing patterns; on average, concept cells respond to about 2-3% of the stimulus set, with firing maintained to similar, related concepts. This observation contrasts with predictions made by both highly distributed connectionist models (e.g. McClelland et al., 1995) and fully localist accounts, e.g. that of the hypothetical ‘grandmother cell’ (i.e. a single cell that codes for a concept, Gross, 2002) at the other extreme. Though difficult to disprove with existing single-cell recording techniques, a ‘one neuron per concept’ account is highly unlikely. Namely, the chances of recording the one active neuron encoding the precise exemplar in the experiment’s stimulus set (e.g. Jennifer Aniston) are minuscule. In addition, it would be a highly vulnerable system, since the loss of one neuron could entail the loss of a concept. Rather, sparse coding networks fall somewhere in between fully distributed and fully localist models. Waydo (2006) developed a method for obtaining a probability distribution of sparseness based on Quian Quiroga’s (2005) data. He concluded that, with an estimated five million (out of 10^9) MTL neurons being activated by a typical stimulus, each MTL neuron will respond to approximately 50-150 distinct representations.

Hence, intracranial recordings in patients do show convincing evidence for the existence of cells with explicit invariant conceptual representation. However, one shortcoming of this technique is that electrode placement is restricted to purported epileptic foci. Therefore, the question remains whether conceptual representations are limited to the MTL.

Neuropsychological and task-based fMRI studies have implicated areas beyond the MTL in categorization processes, such as prefrontal cortex and posterior cingulate (Freedman, 2001; Dronkers et al. 2004; Binder et al., 2009). As intracranial recordings in healthy participants are impossible for ethical reasons, non-invasive imaging techniques such as fMRI are required to study the nature of conceptual representations in the brain. Here, we aim to investigate whether distributed small-scale ensembles of concept representations, first discovered at the single-cell level, can be detected with fMRI at the systems level in healthy participants’ MTL and beyond. Not restricting the analysis to any particular brain region, we can potentially discover all brain areas implicated in conceptual representation.

We used Representational Similarity Analysis (RSA, Kriegeskorte, 2008), a multivariate pattern analysis method, which tests how well predicted similarities between stimuli are reflected in the similarities of brain activation patterns evoked by these stimuli. RSA has been successfully used in studies investigating how categories are organized in abstract representational space in both humans (Connolly et al, 2012; Kiani et al., 2007; Devereux et

al., 2013; Simanova et al., 2013) and non-human primates (Kriegeskorte, 2008). These studies generally agree with findings of classification studies on category representations (Haxby et al., 2001; Spiridon & Kanwisher, 2002; Cox & Savoy, 2003; O'Toole et al., 2005; Reddy & Kanwisher, 2007; Op de Beeck et al., 2010; Brants et al., 2011). They demonstrate that multivariate analysis techniques can probe the population responses representing complex visual stimuli in the ventral visual stream. Many of these studies have used categories such as faces, animals, objects and scenes, for which a plethora of studies using classical activation mapping has shown dissociations between their loci of activation (Martin et al., 1996; Epstein & Kanwisher, 1998; Chao et al., 1999; Chao & Martin, 2000; Kanwisher, 2010).

We build on and extend this work by including stimuli from these four widely studied categories (faces, animals, objects, scenes), which additionally belong to one of two superordinate concepts. We use the highly popular fantasy universes of *Harry Potter (HP)* and *Lord of the Rings (LotR)* as the superordinate conceptual representations. Following the discovery of 'concept cells', we hypothesize such concepts could be stored in sparse networks in the MTL (Quiñones Quiroga, 2012). If the MTL, or any other region, contains information about concepts, the RSA should yield higher within-concept representational similarity than across-concept representational similarity, across all four categories. Because probing these small-scale ensembles benefits from high spatial resolution, as well as high signal-to-noise ratio (SNR), we used high-field fMRI at 7-Tesla. Participants were scanned while viewing pictures of four different categories (faces, animals, objects & scenes) from either *HP* or *LotR* while performing an orthogonal category judgment task on each stimulus. Using this design, we shed light on the representational content of both categorical object representation (replicating earlier findings at 7T) and conceptual representations.

Methods

Participants

Sixteen healthy participants (mean age = 26.1 years, SD = 8.6, 9 females) participated after providing written informed consent in accordance with the Declaration of Helsinki and the local ethics board. All participants had normal hearing and normal or corrected-to-normal vision and were selected based on their knowledge of the *Harry Potter* and *Lord of the Rings* series, with only those with excellent familiarity (having read all books and seen all movies) being included. Participants received a monetary reward for participation. The study was approved by the local ethics committee (CMO region Arnhem/Nijmegen).

Stimuli

We selected 107 pictures from movies belonging to the *Harry Potter* and *Lord of the Rings* superordinate concepts (henceforth named “concepts”). We then tested whether a separate set of participants, who had also seen all movies and read all books of both series (N = 11), could accurately identify them as belonging to either concept by having them name the objects depicted. Participants saw the pictures for two seconds, matching the stimulus presentation to the MRI scanning task. We used open questions to greatly reduce the number of false positives by chance, as compared to a forced choice test between *HP* and *LotR*. The responses were scored as either correct or incorrect. Out of the best recognized pictures, we picked six for each of one semantic category (“category”: faces, animals, objects and scenes) for both concepts (the fantasy worlds of *Harry Potter* or *Lord of the Rings*), resulting in a total of 48 stimuli. Recognition accuracy for each category ranged from 91% to 95%, with no significant differences between categories ($F(3,40) = 0.095, p = 0.962$) nor concepts ($F(1,40) = 0.571, p = .454$).

Stimuli were converted to black-and-white, resized to 400 x 400 pixels and matched on their low-level features (luminance, contrast and spatial frequency) using the SHINE toolbox (Spectrum, Histogram and Intensity Normalization and Equalization, Willenbockel et al., 2010) to avoid confounding the contribution of low- and high-level processing across stimulus categories.

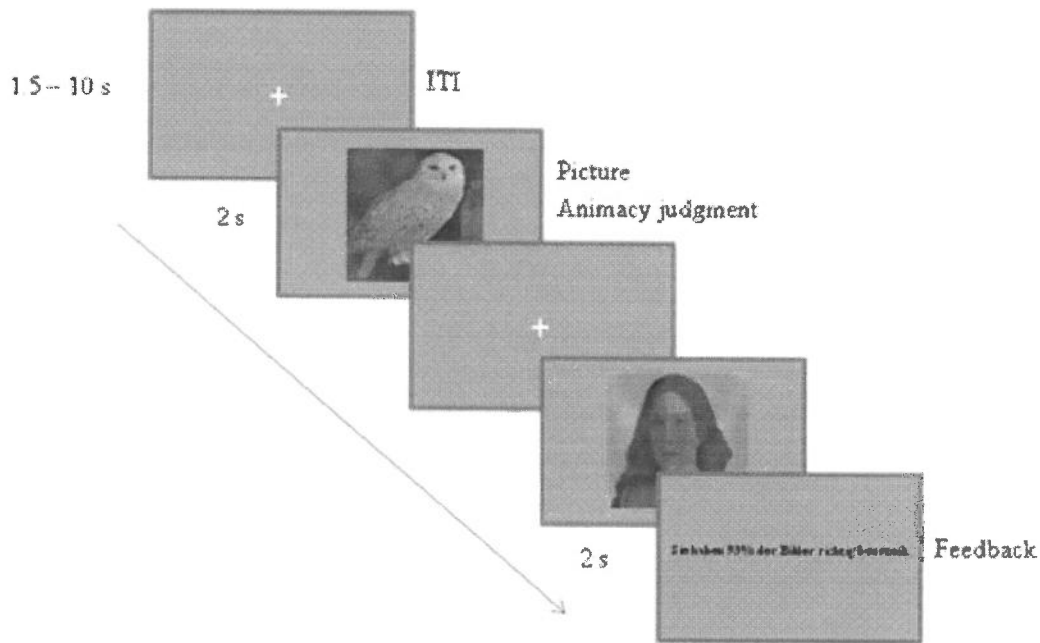


Fig. 1 Experimental task. Example of trial sequence for a scanning session. Participants were instructed to make an animacy judgment (press right or left button) for every stimulus.

Experimental design

Before the study, participants filled an online questionnaire in which they rated their familiarity with the two series on a 10-point scale.

Stimuli were presented in eight blocks of approximately six minutes with breaks of twenty seconds in between. During each block, all pictures were presented one by one (stimulus duration was 2 s, ITI was randomized with $M = 5s$, $SD = 1$, range 1.5-10s). A red dot was overlaid at the center of the screen. Participants were instructed to maintain fixation on the red dot throughout the experiment. The order of the stimuli was randomized across participants. On each trial, participants indicated whether the object in the picture was animate or inanimate by button presses with their right index and middle finger. At the end of each block, feedback about the participant's accuracy on the animacy task was presented. The button mapping of the animacy task was counterbalanced across participants. We collected reaction times (RTs) and accuracies of the animacy task during the task session.

After the fMRI session, participants were asked to arrange the pictures according to how similar they perceived them to be by letting them place the objects in a two-dimensional arena (Kriegeskorte & Mur, 2012, see Fig. S2). They were instructed to drag-and-drop the stimuli on a computer screen and to place stimuli they perceived to be similar more closely to each other than those they found more dissimilar. This was done in rounds, with all 48 stimuli

present in the arena at first. After the first round, a different subset of stimuli was shown on each round until the task time ran out after 15 minutes. Based on these iterative similarity judgments of all items, a stimulus-by-stimulus distance matrix was computed. Fourteen participants completed the arena task. We tested whether participants would group the stimuli according to the concept they belonged to, and/or according to category membership.

FMRI data acquisition

Participants were scanned with a Siemens 7T MRI-scanner at the Erwin L. Hahn Institute for Magnetic Resonance Imaging (Essen, Germany), using a 32-channel surface coil. T1-weighted structural images from each subject were acquired using the MP2RAGE (3D magnetization-prepared rapid gradient echo, Marques et al., 2010) scanning protocol with the spatial resolution of 0.75 mm isotropic. A field map for distortion correction was recorded before starting the functional scans using a gradient echo sequence.

Blood-oxygenation-level-dependent (BOLD) T2*-weighted functional images were acquired using a three-dimensional echo-planar imaging (EPI) pulse sequence (Poser et al., 2010) with a TR of 2.224 s and isotropic resolution of 1.5mm (80 slices). To allow for T1 equilibration, three (N = 11) or seven (N = 5) dummy volumes were discarded before the main scan. The scanning sessions were subdivided into two runs of four blocks each, with a duration of approximately 27 minutes per run.

Behavioral data analysis

Participants' differences in familiarity between *HP* and *LotR*, as assessed by pre-study familiarity ratings, were tested using a 2-tailed t-test. For analysis of the scanning task, only reaction times above 200 ms of correct trials were included. RTs and accuracies of the animacy task were analyzed using a univariate ANOVA and a chi square test, respectively. For analysis of the arena task, we averaged the within-concept/category and across-concept/category distances and tested them against each other using independent sample t-tests. Statistical tests were done using SPSS (IBM SPSS Statistics for Windows, Version 21.0 Armonk, NY: IBM Corp.) and MatLab2012b (The MathWorks, Inc., Natic, MA).

FMRI data preprocessing

The fMRI data were pre-processed using the Automatic Analysis toolbox (<https://github.com/rhodricusack/automaticanalysis/wiki>), implemented in MATLAB R2012b, which combines functions from SPM8 (<http://www.fil.ion.ucl.ac.uk/spm>), FMRIB Software Library v5.0 (<http://fsl.fmrib.ox.ac.uk/fsl/fslwiki/>) and Freesurfer

(<http://surfer.nmr.mgh.harvard.edu/>). Preprocessing included unwarping and realignment of the functional volumes to the first volume of the first run (Andersson et al., 2001).

Compartment signals were extracted and later fed into the general linear model (GLM) as nuisance regressors (Verhagen et al., 2008). Structural volumes were denoised using an Adaptive Optimized Nonlocal Means filter (MRI denoising software package, Coupe et al., 2008) to improve subsequent segmentation and brain extraction. Brain extraction and segmentation of white matter, gray matter and CSF voxels was carried out using FSL functions (Brain Extraction Tool, Smith et al., 2002) and the images were normalized nonlinearly to a group-specific EPI template made with the Anatomical Normalization Toolbox (<http://www.picsl.upenn.edu/ANTS>).

Analysis of fMRI time series

All analyses were carried out on a whole-brain level. Using a GLM, regressors were fitted to the time-series at each voxel. All models estimated included only orthogonal regressors, modeling all trial events and ITIs. Six movement regressors were included in all analyses to model out movement-related physiological noise. The regressors were convolved with the canonical haemodynamic response function (HRF), producing a modeled time-course of neural activity. Univariate analyses were performed on a category representation level (e.g. *scenes > faces, animals & objects*) and on a conceptual level (e.g. *HP > LotR*). Neural activity maps were spatially smoothed with an 8mm FWHM kernel and warped from their native space onto a Montreal Neurological Institute (MNI) template (Fonov et al., 2011).

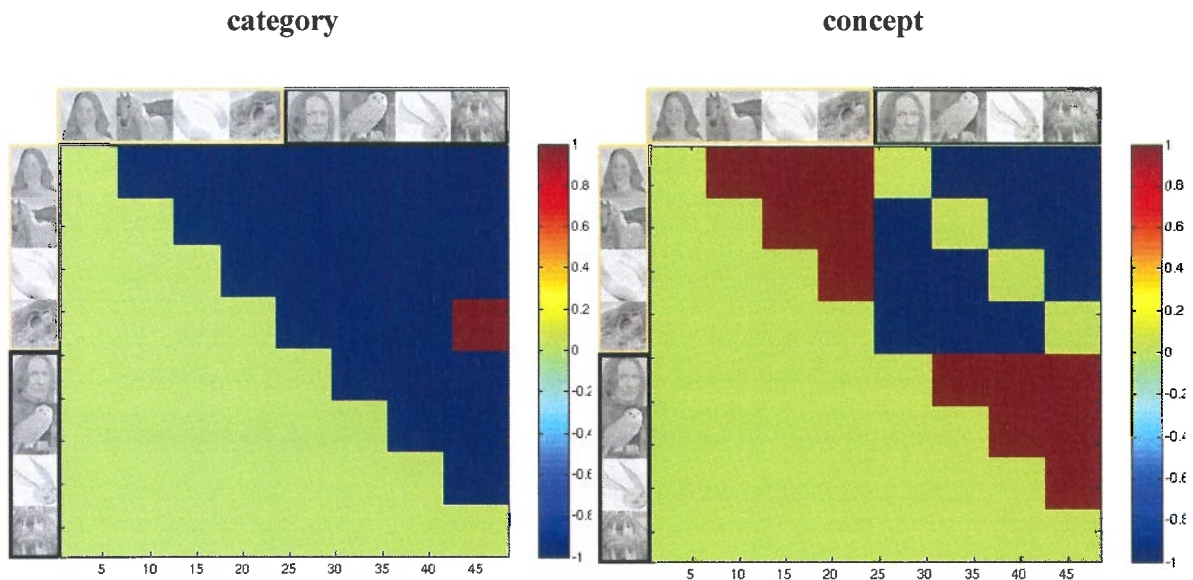


Fig. 2. Experimental rationale. RSA contrast matrices to probe categorical (e.g. about scenes, **left**) and conceptual representations (**right**). Red indicates high similarity, blue indicates low similarity. The diagonal is not included, as the similarity of a regressor to itself would be 1 by definition. By relating the neural data to these predictor matrices, RSA tests how similarities of brain activation patterns are related to predicted similarities between stimuli.

Representational Similarity Analysis

Multivariate pattern analysis (MVPA) takes into account the intrinsically multivariate nature of fMRI data. While univariate analyses are performed on individual voxels, MVPA looks at the pattern of activity across a set of voxels. In this sense, MVPA is “information-based”, rather than “activity-based” (Kriegeskorte, 2008). A particular type of MVPA is Representational Similarity Analysis (RSA, see Fig. 3), which abstracts from the activity patterns themselves by computing representational similarity matrices that contain information about a particular representation in the brain and can be related to theory and behavior by comparing these matrices (Kriegeskorte, 2008).

To perform RSA, we first modeled the four different categories separately for both concepts yielding a total of eight regressors. We extracted the voxel-wise beta values for each regressor and a brain mask was applied to the images. Searchlight mapping was performed on the native space images of each participant by moving a spherical ROI of 3 voxel radius (4.5 mm) through the gray-matter masked volume one voxel at a time. Resultant statistics were mapped back to the center voxel of each spherical ROI yielding single-subject information maps. The analysis was restricted to searchlights that contained at least 30 voxels. The pattern of beta values of every regressor contained in every sphere was correlated with that of the remaining regressors, resulting in twenty-eight ($N*(N-1)/2$) unique correlation maps which

were normalized using a Fisher z transform. The normalized correlation maps were averaged and contrasted in two different ways. To test for concept-specific representational similarity, we averaged all twelve unique within-concept comparisons and all sixteen across-concept comparisons and subtracted the resulting ‘across’-correlations from the ‘within’-correlations. Similarly, contrasts were constructed to test for higher representational similarity for the four categories by contrasting within-category correlation maps with between-category correlation maps for every category separately. Finally, we contrasted the averaged correlation maps for *faces* and *animals (animate)* against those for *objects* and *scenes (inanimate)*, yielding six contrasts in total. To perform group level statistics for each of these RSA contrasts, we performed a non-parametric permutation test using 5000 permutations on the resulting six images using `fsl_randomise` (Winkler et al, 2014).

Results

Behavioral results

Familiarity

Participants' pre-study familiarity rating, as tested with a 2-tailed paired t-test, was slightly higher for the *Harry Potter* series ($M = 7.74$) than for *Lord of the Rings* ($M = 6.89$, $t(15) = 2.599$, $p = .015$).

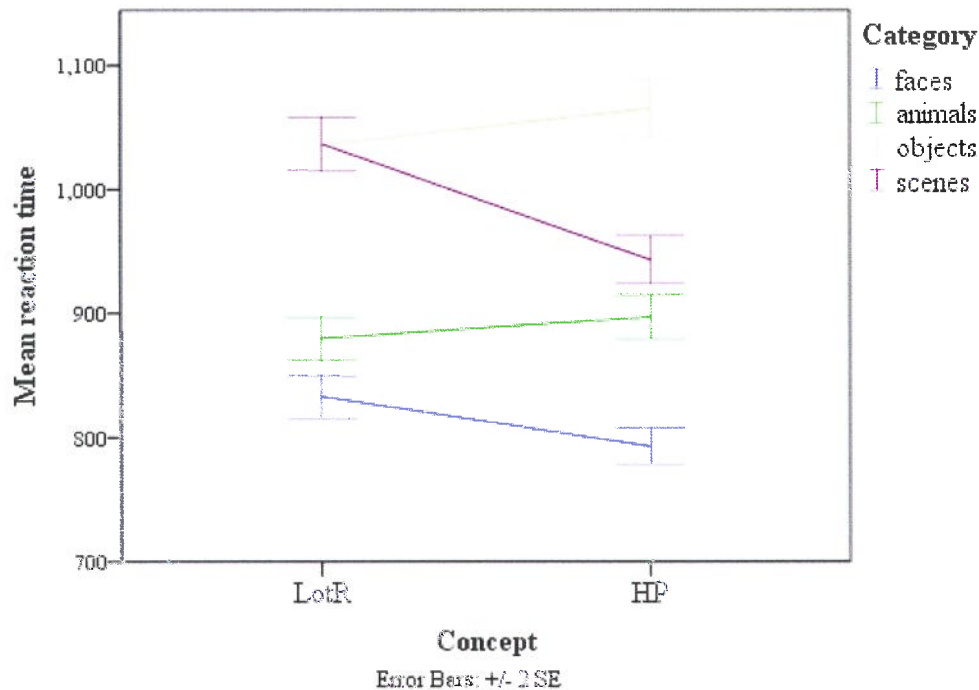


Fig. 3 Mean reaction time. Category had a main effect on reaction time. Participants were faster for *faces*, followed by *animals*, *scenes* and *objects*. A significant interaction between the category and concept is also shown.

Reaction time

For reaction time, we found no significant main effects of *concept* ($F(1, 15.5) = 3.77$, $p = .070$). However, reaction times (RTs) differed between *categories* ($F(3, 45.5) = 54.16$, $p < .001$, $\eta^2 = .781$). On average, participants tended to react fastest to *faces* ($M = 812.67$ ms, $SD = 69.13$), significantly faster than to *animals* ($M = 891.63$, $SD = 81.79$; $t(15) = -6.69$, $p < .001$). In turn, *objects* ($M = 1061.60$, $SD = 110.54$) had slower RTs than animals ($t(15) = -8.95$, $p < .001$). Participants' RTs to *scenes* ($M = 995.94$, $SD = 121.29$) were slowest and, again, significantly slower than to objects ($t(15) = 2.51$, $p = .024$).

In addition to the main effect of *category*, the two factors interacted significantly ($F(3, 46.6) = 12.72$, $p < .001$, $\eta^2 = .450$), as can be seen in Fig. 3.

Accuracy

No significant difference in the frequency of correct versus incorrect animacy judgments was found for the different concepts ($\chi^2 = 0.3117, p = .577$). However, participants were more accurate for some categories than for others ($\chi^2 = 46.5302, p < .001$): the accuracy pattern resembled that of the RTs, with faces being judged most accurately, followed by animals, then scenes and objects.

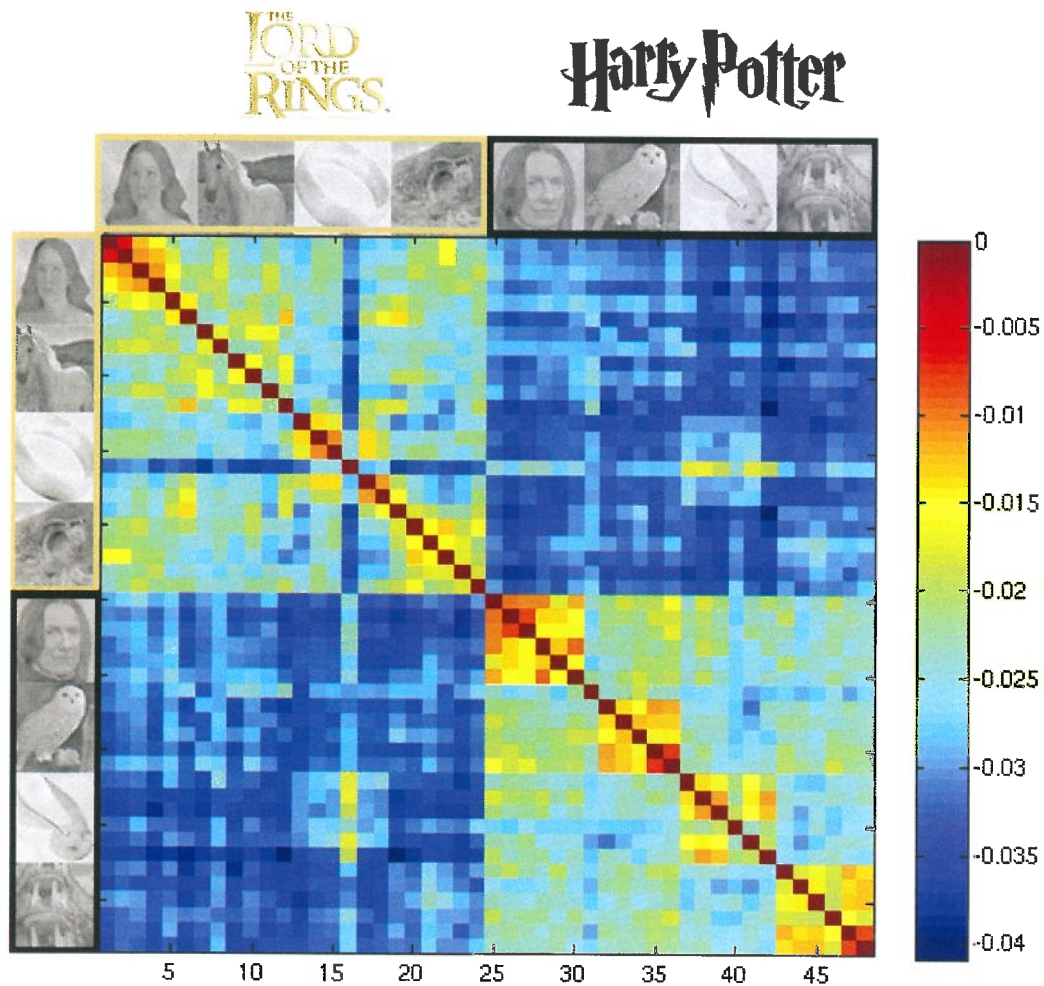


Fig. 4 Mean arena task distance matrix obtained from averaging across all participants showing the separability of conceptual and categorical information in behavior. Within-concept distance is smaller than across-distance. Category-clusters can also be observed.

Arena task

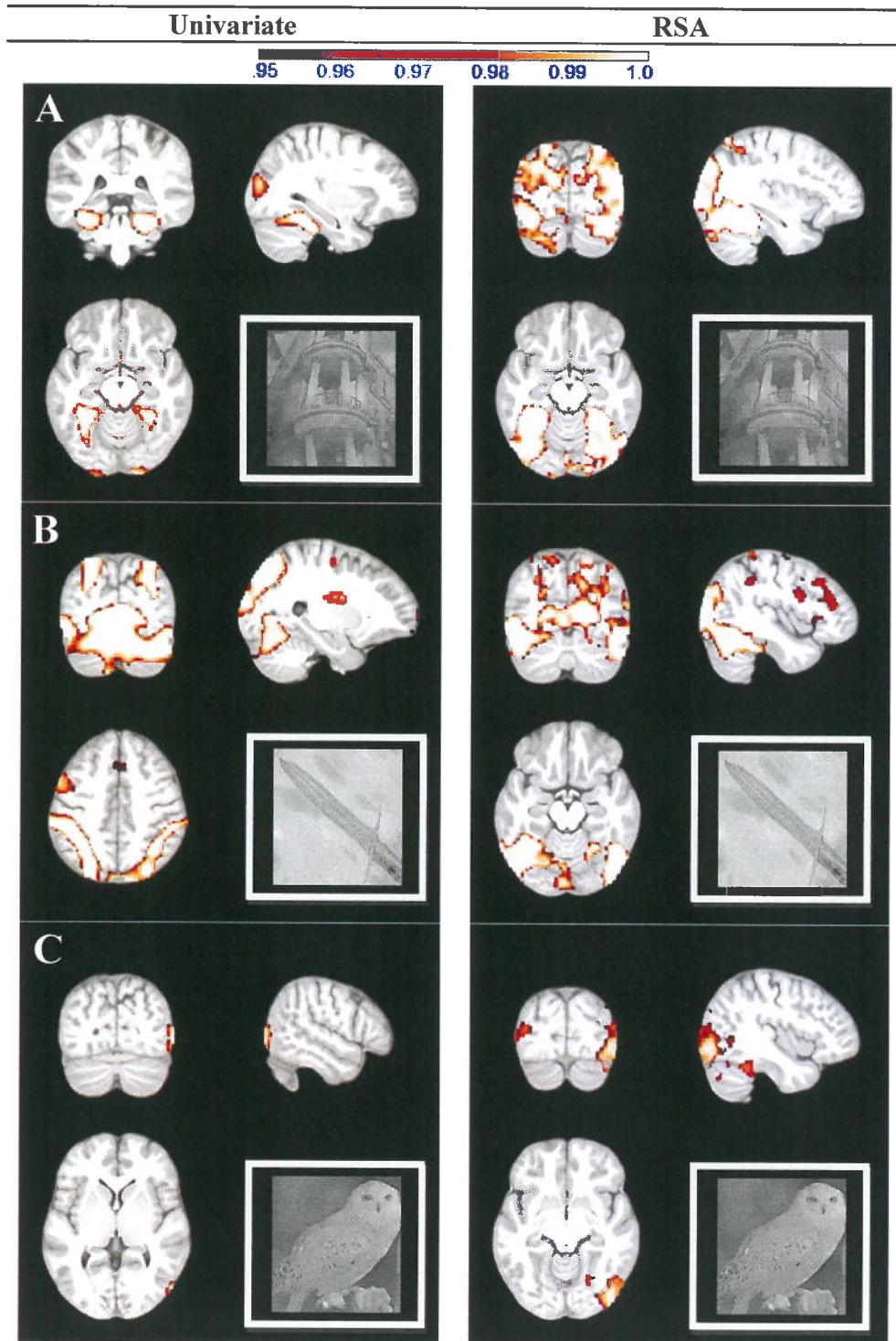
Within-concept item distance ($M = -0.0227, SD = 0.0049$) was significantly smaller than across-concept item distance ($M = -0.0318, SD = 0.0033; t(1102) = -36.32, p < .001$) showing that participants grouped the stimuli according to concepts.

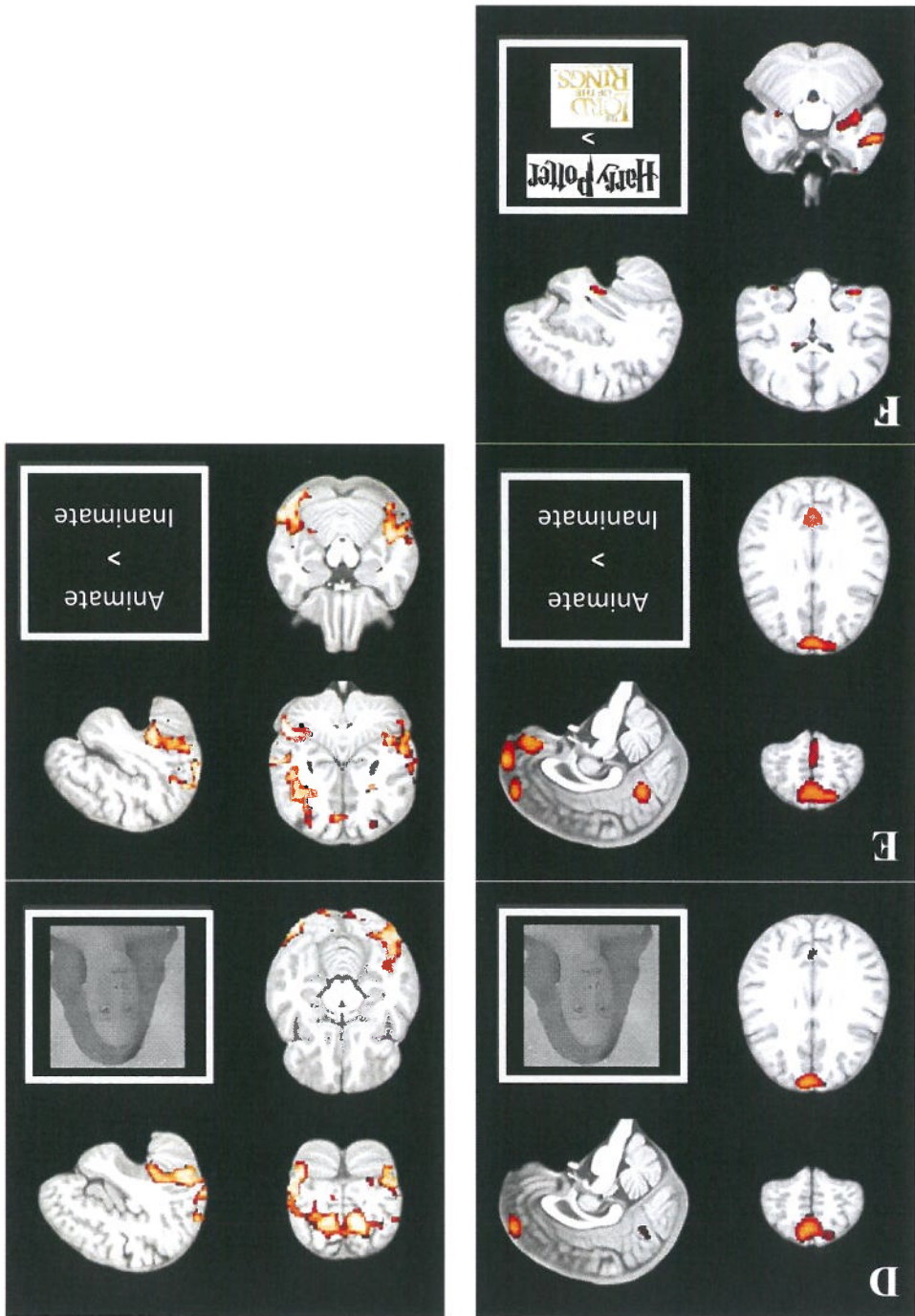
For category-specific clusters, we tested the within-category distance of each category against the mean across-category distance ($M = -0.0284$, $SD = 0.0052$). This showed that faces ($M = -0.0222$, $SD = 0.0085$) were clustered together ($t(922) = 8.41$ $p < .001$), as were animals ($M = -0.0242$, $SD = 0.0075$; $t(922) = 5.82$ $p < .001$), objects ($M = -0.0228$, $SD = 0.0069$; $t(922) = 7.7737$, $p < .001$) and scenes ($M = -0.0231$, $SD = 0.0072$; $t(922) = 7.31$, $p < .001$). These effects can be seen in the mean distance matrix of the arena task results (Fig. 4).

Table 1. Summary of contrasts for univariate analyses reported.

| Name | Contrast | |
|----------------|--------------------------|-----------------------------------|
| <i>Scenes</i> | <i>scenes</i> | > <i>faces, animals, objects</i> |
| <i>Objects</i> | <i>objects</i> | > <i>faces, animals, scenes</i> |
| <i>Animals</i> | <i>animals</i> | > <i>faces, objects, scenes</i> |
| <i>Faces</i> | <i>faces</i> | > <i>animals, objects, scenes</i> |
| <i>Animacy</i> | <i>faces, animals</i> | > <i>objects, scenes</i> |
| <i>Concept</i> | <i>Harry Potter</i> | > <i>Lord of the Rings</i> |
| | <i>Lord of the Rings</i> | > <i>Harry Potter</i> |

Imaging results





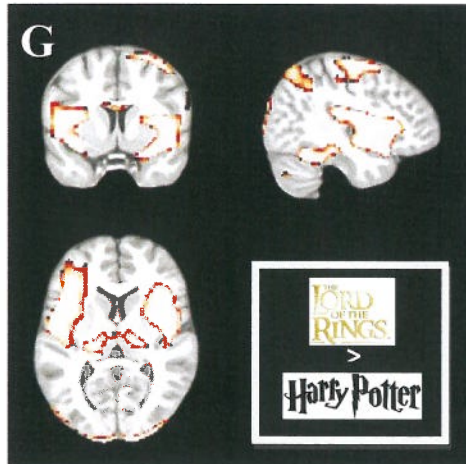


Fig. 5 Univariate and multivariate imaging results. Significant effects are shown at $\alpha = .05$, cluster-corrected. Colorbar: $1-p$. **Left** BOLD activation maps in the sagittal, coronal and horizontal plane. **Right** Neural pattern similarity maps in the sagittal, coronal and horizontal plane. **A.** *Scenes* selectively activated the occipital cortex, the parahippocampal and fusiform gyri, cuneus, precuneus and the calcarine sulcus (**left**), while the RSA effect was widespread along the visual stream and showed significant overlap with the *objects* RSA effect (**B. right**). **B. Left** Objects univariate effects were located along the dorsal visual stream, in addition to the MTL. **C.** Although *animal*-selective voxels were restricted to a small cluster in the right middle occipital gyrus (**left**), there were more regions that showed higher pattern similarity for this category (**right**). **D.** Surprisingly, no BOLD effect was found in the fusiform gyrus for the *faces* contrast (**left**), but this region did contain information about faces in the RSA (**right**). **E.** Similarly, the regions showing significant univariate and multivariate effects for animacy, respectively, showed little overlap with RSA effects located mostly along the ventral visual stream (**right**) while BOLD signal change was significant in several frontal regions (**left**). **F.** On a conceptual representation level, despite univariate differences in activation levels for the contrast *HP > LotR* showing activation in the MTL (**left**), the visual cortex and frontal cortex, there were no brain areas with higher within- than across concept pattern similarity (not shown). **G.** Control analyses will examine whether a shift in the t-distribution might underlie the massive activations observed for the contrast *LotR > HP*.

Category representation

According to the modularity hypothesis (Fodor, 1983), object representations are characterized by category specificity, predicting that differential BOLD activations should be found for the four categories presented. Therefore, we first ran univariate GLMs to reveal higher activity levels associated with representations at the categorical level. An overview of all univariate contrasts revealing significant activation can be found in Table 1. All results presented are significant at $\alpha = .05$, cluster corrected using threshold-free cluster enhancement (Smith & Nichols, 2009). Statistical results can be found in detail in the supplementary material. Cerebral labeling was based on the Automated Anatomical Labeling Atlas for SPM 8 (Tzourio-Mazoyer et al., 2002). First, we investigated whether we could dissociate different category-selective regions along the visual ventral and dorsal streams that are uniquely activated by different categories by contrasting beta values from one category against those of all other categories. We indeed found differential activation profiles for the four categories presented.

When viewing **scenes** (Fig. 5A, left), the visual cortex and the fusiform gyrus became activated bilaterally. This activation included the right cerebellum and the left parahippocampal place area (PPA), an MTL structure known to be especially responsive to scenes (Epstein et al., 1999). In addition, another peak of activation was found in the right calcarine sulcus, extending into the cuneus and precuneus (see Table S1).

While scenes activation was localized mostly along the ventral visual stream, the contrast for **objects** (Fig. 5B, left) revealed clusters of activation with greater overlap with the dorsal stream (Goodale & Milner, 1992). These included voxels in the left lingual gyrus extending dorsally into the left precentral gyrus, the bilateral supplementary motor area, the bilateral inferior frontal cortex, orbital part, right inferior frontal cortex, triangular and left middle and superior frontal gyri. Small clusters of activation were also found in the right cerebellum and the left superior temporal gyrus (see Table S2).

Voxels with higher activity levels for **animals** (Fig. 5C, left) were restricted to a small cluster in the right middle occipital gyrus (see Table S3).

Surprisingly, no fusiform activation was found when testing the **faces** contrast (Fig. 5D, left). Activation of the fusiform face area (FFA) has been found consistently in previous work on face perception (Kanwisher et al., 1997). Instead, we found activation in the right medial superior frontal gyrus (See Table S4).

Given the fact that the scenes contrast (Fig. 5A, left) activated the FFA, in addition to the PPA, and the face contrast failed to activate it, we decided to test a post-hoc contrast *faces > animals & objects*. As some scene stimuli also contained human faces, their neural response might not be purely 'scenic', but also contain a face-responsive signal. However, although the scenes regressor might have explained some of the variance for faces, leading to a weakened face contrast, *faces > animals & objects* also failed to reveal a significant effect in the fusiform gyrus.

Activity for **animate** stimuli (*faces & animals*) was higher than that for inanimate stimuli (*objects & scenes*, Fig. 5E, left) in the left medial orbitofrontal and superior medial frontal gyri, the precuneus and the right middle temporal gyrus (see Fig. S5)

We then asked whether we could identify brain areas that show higher similarity associated with the four categories. The RSA revealed widespread regions containing categorical information. Categorical information was evident along most of the ventral visual stream.

While all categories were represented in multiple brain areas, relatively few showed higher similarity for **animals** than for other categories (Fig 5C, right & Table S6). In line with the univariate results (Fig 5C, left), this was found to be true for voxels in the right inferior and bilateral middle occipital gyrus. In addition, however, the bilateral calcarine sulcus and the bilateral precuneus, as well as the left superior occipital and middle temporal gyri showed an RSA effect for animals, in absence of univariate differences.

Similar to their univariate effects, the RSA effects for **scenes** (Fig. 5A, right) and **objects** (Fig. 5B, right) showed significant overlap. Both categories showed significant representational similarity in large parts of the ventral visual stream. These areas including the bilateral calcarine sulcus, extending ventrally along the lingual and fusiform gyri, and spreading dorsally via the middle occipital gyrus, posterior and middle cingulum and precuneus to the inferior parietal lobule. All these areas were found to contain information about both scenes (see Table S7) and objects (see Table S8). However, for the object RSA contrast, significant regions in the RSA extended further dorsally into the superior parietal lobe, medial and superior frontal gyri and supplementary motor area bilaterally. This is consistent with findings implicating the dorsal stream in the representation of man-made objects (Chao & Martin, 2000). While the supplementary motor area also contained information about scenes, this cluster was much smaller than that found for objects.

While the precuneus and right superior parietal gyrus also contained information about **faces**, no other dorsal regions showed an RSA effect for this category (Fig. 5D, right). In the ventral stream, however, the middle occipital and fusiform gyri, as well as cerebellum, were again found to contain information about this category (see Table S9), in absence of a univariate effect in these regions (Fig. 5D, left)

Brain areas with significant pattern similarity for **animacy** (Fig. 5E, right) were found to include the right calcarine sulcus and lingual gyrus, the left middle cingulum, caudate and thalamus, in addition to an RSA effect in the right middle and left superior frontal, left superior parietal and the right parahippocampal gyri (see Table S10).

Concept representation

We again first looked at differences in BOLD activation associated with conceptual knowledge. Here, we found several regions in the MTL, visual cortex and motor cortex to be more active for pictures of *HP* compared to *LotR* (Fig. 5F). Activations in the MTL included the anterior part of the parahippocampal gyrus (i.e. perirhinal cortex) bilaterally, the left

superior temporal and the right fusiform gyri. The posterior activation spanned the left calcarine sulcus while the right caudate, and precentral and left inferior orbitofrontal gyri, were activated in the more dorsal regions (see Table S11). We then contrasted *LotR* against *HP* and observed massive clusters of activation throughout the brain. Given that most extensive cluster spanned almost 40,000 voxels (see Table S12), skepticism towards the origin of these activations is warranted. A shift in the t-distribution of the *HP* or *LotR* activation maps might explain these findings.

We then tested whether we could probe the hypothesized sparse networks representing conceptual knowledge. However, despite the univariate differences in activations levels, the RSA contrast for **concepts** did not show significant voxels, suggesting that there were no brain areas that showed higher within- than across-concept pattern similarity.

Discussion

Determining how mental representations map onto patterns of neural activity is a key challenge for cognitive neuroscience. In this study, we aimed to shed light on the representational content on a categorical and conceptual level, replicating and extending previous work on semantic representations by introducing categories belonging to superordinate concepts. Using multivariate analysis tools at high-field, we tried to find evidence for the existence of sparse networks of concept cells at the systems level, while also replicating studies on category-selective regions in the visual pathway. To the best of our knowledge, this is one of the first studies using RSA at 7-Tesla. RSA identified widespread regions underlying semantic representations on a categorical level replicating earlier findings. While RSA was not able to distinguish between concepts in any brain region, univariate results suggest a possible role of the perirhinal cortex in the processing of conceptual knowledge.

We started by asking if we could identify the same neural correlates of category-specific knowledge that have been reported consistently in the past two decades. We did observe differential BOLD activations in response to faces, animals, objects and scenes. Scene stimuli elicited activation in the PPA, which occupies the most posterior portion of the medial temporal lobe (Epstein & Kanwisher, 1998) and has been found to be reliably activated in virtually every participant when viewing pictures of scene stimuli (Epstein & Kanwisher, 1998; Litman et al., 2009). In addition to the PPA, scenes activated more widespread areas in the ventral MTL. It has been found that category-specific regions are rarely silent to other

object categories, but rather show a smaller response. As most studies reporting PPA activation for scenes have been carried out on 1.5 or 3 Tesla scanners, the increase in SNR brought about by moving to 7-T might explain why more anterior portions of the parahippocampal gyrus are activated by scenes in this study, but not in previous ones. This suggests that object representations in the ventral occipito-temporal cortex are not limited to a discrete area, but rather are widespread and overlapping, a notion that we will address later.

We found the PPA, in addition to the fusiform and lingual gyri, to also be activated by objects, replicating effects reported by multiple research groups (Martin et al., 1996; Mummary et al., 1996; Cappa et al., 1998; Chao et al., 1999; Moore & Price, 1999). More recently, Litman et al. (2009) also reported parahippocampal activity associated with objects; however, they found a double dissociation between scene- and object-selective voxels with objects activating more anterior portions of the parahippocampal gyrus, i.e. the perirhinal cortex. The reason why we did not find evidence for the dissociation between scenes and objects may be due to the fact that stimuli were matched on their low-level features, reducing perceptual differences between categories. This notion is supported by reports that objects are also represented according to perceptual properties such as visual shape, in addition to their semantic properties (Edelman et al., 2008). The perirhinal cortex may be sensitive to these perceptual features, as it has been found to enable fine-grained distinctions between objects (Buckley et al., 2001; Bussey &aksida, 2002; Moss et al., 2005; Taylor et al., 2006, 2009; Barense et al., 2010; Mion et al. 2010; Kivisaari et al., 2012), This raises the possibility that activity in the regions reported by Litman et al. (2009) was mainly driven by sensory attributes of the objects, rather than their category membership per se. In addition to the MTL, we also found regions along the dorsal visual stream (i.e. in the supplementary motor area and the precentral gyrus) to respond to objects, consistent with the idea that information about objects is stored according to their features and attributes such as form (in the ventral temporal cortex) and their associated specific hand movement (in motor cortex, Chao & Martin, 2000).

Animal-specific activations have been found less consistently, with some studies finding activations in the calcarine sulcus (Martin et al., 1996; Chao et al, 2002), the posterior region of the superior temporal sulcus (Chao et al, 1999, 2002), the lateral fusiform gyrus and the middle occipital gyrus (Chao et al, 2002). Here, we found only the middle occipital gyrus to be preferentially active when viewing animals. A possible explanation for this less widespread activation could be the fact that our animal stimuli, given their nature as fantasy

beings, might not consistently be treated as animals by the brain. In fact, only five out of twelve animal stimuli depicted real, existing animals, while others included beings such as dragons or living trees. Hence, failure to replicate more widespread findings along the occipito-temporal region might simply reflect either a lack of statistical power or a lack of specificity in the stimuli.

A surprising finding was the absence of fusiform activation in response to face stimuli. The FFA, like the PPA, is among the most reliably found ‘functional localizers’ (Kanwisher et al., 1997, 2010; Kanwisher & Yovel, 2006). We instead found activation in the medial superior frontal gyrus, which has been found in some earlier studies (Henson et al., 2003; Zhang et al., 2009). This region has been proposed to be part of an ‘extended’ network for face processing, theorized to prepare the brain to process faces that one is likely to encounter in their environment (Bar et al., 2008; Zhang et al., 2009). Again, differences in the stimuli’s low-level features might explain this effect.

Abstracting from single categories, we tested whether we could find activity associated with animacy. The frontal activation that we found for animate versus inanimate stimuli showed overlap with activations found for faces. This is in itself not surprising, as the face stimuli were a subset of the animate set. Some studies have argued for a distinction between domain-specific knowledge systems for animate and inanimate objects, based on neuropsychological findings (Warrington & Shallice, 1984; Caramazza & Shelton, 1998), arguing that animate and inanimate objects are somehow processed differently. Seemingly in line with this explanation, Kriegeskorte (2008) also found that the inferior temporal gyrus of both monkeys and humans showed higher neural similarity within animate and inanimate stimuli relative to across animacy comparisons between stimuli, a finding that we replicated here. However, this finding does not necessarily imply different neural systems underlying the processing of these two types of objects. Rather, we argue that these objects are represented in one conceptual space, possibly in the MTL, with the RSA simply showing that, on average, animate objects are represented closer to each other than to inanimate objects. Ilic et al. (2013) argued that, rather than animacy per se, it is the differences in intra-item variability between animate and inanimate objects that account for differences in the behavioral response to these two classes of stimuli. In other words, animacy effects such as differences in processing speed can be explained by the fact that animate objects tend to have lower intra-item variability than inanimate ones. This, and the absence of a univariate effect of animacy in the MTL, the place

where these object representations may be stored, argues against the existence of separate neural systems for animate and inanimate objects.

Comparing the univariate results with the RSA effects, we showed that even though specific responses were found for only a subset of categories using univariate analyses, RSA analyses demonstrated that all categories are represented along the ventral visual stream. First, this supports the finding that multivariate measures can pick up information that is missed by classical activation mapping (Haxby et al, 2001; Kriegeskorte, 2008). Second, it shows that category information is represented in a distributed manner, along the MTL and beyond, and is not restricted to category-specific areas reported in the literature for two decades. Regions such as the PPA do not appear to be dedicated to representing solely spatial arrangements, for example, but rather contain information relevant for the representation of all objects.

The second research question was whether we could identify the neural substrates of the superordinate representation of the four categories, i.e. the concepts of *Harry Potter* and *Lord of the Rings*. Although the *LotR* versus *HP* contrast did reveal massive clusters of activation throughout the brain, these results are difficult to interpret. Analysis of the t-distributions will reveal possible shifts in the distribution. If shifted, we will reanalyze the data after normalization. For the reverse contrast, we found the perirhinal cortex to show more activity for *Harry Potter* compared to *Lord of the Rings*. This effect was not driven by perceptual features or differences in categorical content, as all stimuli were matched on their low-level features and the concept contrast was pooled across categories. Although the concept RSA did not yield significant results, this finding suggests that the perirhinal cortex may play a role in the identification of category-invariant superordinate concept representations. Several studies have implicated the perirhinal cortex in familiarity-based recognition memory (Brown & Aggleton, 2001; Henson et al., 2003; Diana et al., 2007). Might the concept effect merely be driven by differences in familiarity between the two concepts? After all, participants did report to be slightly more familiar with *Harry Potter* than with *Lord of the Rings*. While the ‘binding of item and context’ (BIC) model (Diana et al., 2007) predicts deactivations of the perirhinal cortex during item retrieval to the degree that the item is familiar, however, we found higher activity for *HP* than *LotR*, arguing against this explanation. More studies are needed to understand the contribution of the perirhinal cortex to conceptual knowledge representations, as higher activity levels could reflect several different processes. Conceptual knowledge could be stored in the perirhinal cortex itself or could be represented elsewhere, but be indexed by the perirhinal cortex upon retrieval. Increasing the number of participants

will be a critical step in making sure the concept RSA is sufficiently powered to detect this (arguably small) effect. The fact that participants did sort the stimuli into two overarching concepts in the arena task makes it more likely that a neural similarity effect will be found (Davis & Poldrack, 2013), as was the case with the categorical knowledge. In this case, this null finding is likely to be trumped by increases in statistical power.

Rather than due to the limited amount of datasets, the reason for the observed null effect could be found in the saliency of our concepts used here. It might be that, in contrast to the categories, which arguably hold an evolutionary relevance for people, the concepts that we used might not have been salient enough to trigger a memory response in participants. In this case, individual participants' "preferential stimuli" would have to be piloted. While Quiñones Quiroga (2005) was able to use the single-cell response as a kind of golden standard to determine which stimuli to include in the probe set, it is unclear what criterion to base stimulus selection on in healthy participants. In addition, it may be crucial to further control the participants' level of motivation and attention between concepts, as these factors might dominate the haemodynamic response and thereby overrule the response of sparse networks via volume transmission (Agnati et al., 1995; Logothetis, 2008).

In conclusion, we show that category-specific information is present along most of the ventral visual stream, arguing against a modular view of category representation in the cortex and present preliminary evidence that the perirhinal cortex may distinguish between category-invariant superordinate concept representations.

References

- Agnati, L., Zoli, M., Stromberg, I. & Fuxe, K. (1995). Intercellular communication in the brain: wiring versus volume transmission. *Neuroscience*, 69, 711-726.
- Andersson, J. L. R., Hutton, C., Ashburner, J., Turner, R. & Friston, K. (2001). Modeling Geometric Deformations in EPI Time Series. *Neuroimage*, 13, 903-19.
- Bar, M., Aminoff, E. & Ishai, A. (2008). Famous faces activate contextual associations in the parahippocampal cortex. *Cerebral Cortex*, 18, 1233-1238.
- Barendse, M., Rogers, T., Bussey, T., Saksida, L. & Graham, K. (2010). Influence of conceptual knowledge on visual object discrimination: Insights from semantic dementia and mtl amnesia. *Cerebral Cortex*, 20, 2568-2582.
- Barsalou., Simmons, W., Barbey, A. & Wilson, C. (2003). Grounding conceptual knowledge in modality-specific systems. *Trends in Cognitive Sciences*, 7, 84-91.
- Binder, J., Desai, R., Graves, W. & Conant, L. (2009). Where is the semantic system? A critical review and meta-analysis of 120 functional neuroimaging studies. *Cerebral Cortex*, 19, 2767-2796.
- Brants, M., Baeck, A., Wagemans, J., & de Beeck, H.P. (2011). Multiple scales of organization for object selectivity in ventral visual cortex. *Neuroimage*, 56, 1372-1381.
- Brown, M. & Aggleton, J. (2001). Recognition memory: What are the roles of the perirhinal cortex and hippocampus? *Nature Review Neuroscience*, 2, 51-61.
- Buckley, M., Booth, M., Rolls, E. & Gaffan, D. (2001). Selective perceptual impairments after perirhinal cortex ablation. *Journal of Neuroscience*, 21, 9824-9836.
- Bussey, T. & Saksida, L. (2002). The organization of visual object representations: A connectionist model of effects of lesion in perirhinal cortex. *European Journal of Neuroscience*, 15, 355-364.

- Cappa, S., Perani, D., Schnur, T., Tettamanti, M. & Fazio, F. (1998). The effects of semantic category and knowledge type on lexical-semantic access: A pet study. *Neuroimage*, 8, 350-359.
- Caramazza, A. & Shelton, J. (1998). Domain-specific knowledge systems in the brain: The animate-inanimate distinction. *The Journal of Cognitive Neuroscience*, 10, 1-34.
- Chao, L. & Martin, A. (2000). Representation of manipulable man-made objects in the dorsal stream. *Neuroimage*, 12, 478-484.
- Chao, L., Haxby, J. & Martin, A. (1999). Attribute-based neural substrates in posterior temporal cortex for perceiving and knowing about objects. *Nature Neuroscience*, 2, 913-919.
- Chao, L., Weisberg, J. & Martin, A. (2002). Experience-dependent modulation of category-related cortical activity. *Cerebral Cortex*, 12, 545-551.
- Connolly, A., Guntupalli, J., Gors, J., Hanke, M., Halchenko, Y., Wu, Y., Abdi, H. & Haxby, J. (2012). The representation of biological classes in the human brain. *Journal of Neuroscience*, 32, 2608-2618.
- Coupe, P., Yger, P., Prima, S., Hellier, P., Kervrann, C. & Barillot, C. (2008). An optimized blockwise nonlocal means denoising filter for 3-D magnetic resonance images. *IEEE Transactions Medical Imaging*, 27, 425-441.
- Cox, D. & Savoy, R. (2003). Functional magnetic resonance imaging (fmri) “brain reading”: Detecting and classifying distributed patterns of fMRI activity in human visual cortex. *Neuroimage*, 19, 261-270.
- Davis, T. & Poldrack, R. (2013). Quantifying the internal structure of categories using a neural typicality measure. *Cerebral Cortex*, 24, 1720-1737.
- Devereux, B., Clarke, A., Marouchos, A. & Tyler, L. (2013). Representational similarity analysis reveals commonalities and differences in the semantic processing of word objects. *The Journal of Neuroscience*, 33, 18906-18916.

- Diana, R., Yonelinas, A. & Ranganath, C. (2007). Imaging recollection and familiarity in the medial temporal lobe: A three-component model. *Trends in Cognitive Sciences*, 11, 379-386.
- Dronkers, N., Wilkins, D., van Valin, R., Redfern, B. & Jaeger, J. (2004). Lesion analysis of the brain areas involved in language comprehension. *Cognition*, 92, 145-177.
- Edelman, S. (2008). *Computing the mind: How the mind really works*. Oxford University Press.
- Epstein R. & Kanwisher, N. (1998). A cortical representation of the local visual environment. *Nature*, 392, 598-601.
- Epstein, R., Harris, A., Stanley, D. & Kanwisher, N. (1999). The parahippocampal place area: Recognition, navigation or encoding? *Neuron*, 23, 115-135.
- Fodor, J. (1983). *The Modularity of the Mind*. Cambridge, MA: MIT Press.
- Fodor, J. (1998). *Concepts. Where Cognitive Science Went Wrong*. Clarendon Press: Oxford.
- Fonov, V., Evans, A., Botteron, K., Almli, C., McKinstry, R. & Collins, D. (2011), Unbiased average age-appropriate atlases for pediatric studies. *Neuroimage*, 54, 313-327.
- Freedman, D., Riesenhuber, M., Poggio, T. & Miller, E. (2001). Categorical Representation of Visual Stimuli in the Primate Prefrontal Cortex. *Science*, 291, 312 – 316.
- Gärdenfors, P. (2004). *Conceptual Spaces*. Cambridge: The MIT Press.
- Goodale, M. & Milner, A. (1992). Separate visual pathways for perception and action. *Trends in Neurosciences*, 15, 20-25.
- Gross, C. (2002). Genealogy of the “grandmother cell”. *The Neuroscientist*, 8, 512-518.
- Haxby, J., Gobbini, M., Furey, M., Ishai, A., Schouten, J. & Pietrini, P. (2001). Distributed and overlapping representations of faces and objects in ventral temporal cortex. *Science*, 293, 2425–2430.

- Henson, R., Cansino, S., Herron, J., Robb, W. & Rugg, M. (2003). A familiarity signal in human anterior medial temporal cortex? *Hippocampus*, 13, 301-304.
- Henson, R., Goshen-Gottstein, Y., Ganel, T., Otten, L., Quayle, A. & Rugg, M. (2003). Electrophysiological and haemodynamic correlates of face perception, recognition and priming. *Cerebral Cortex*, 13, 793-805.
- Kanwisher, N. & Yovel, G. (2006). The fusiform face area: A cortical region specialized for the perception of faces. *Philosophical Transactions of the Royal Society B: Biological Sciences*, 361, 2109-2128.
- Kanwisher, N. (2010). Functional specificity in the human brain: A window into the functional architecture of the mind. *Proceedings of the National Academy of Sciences*, 107, 11163-11170.
- Kanwisher, N., McDermott, J. & Chun, M. (1997). The fusiform face area: A module in human extrastriate cortex specialized for face perception. *The Journal of Neuroscience*, 17, 4302-4311.
- Kiani, R., Esteky, H., Mirpour, K. & Tanaka, K. (2007). Object category structure in response patterns of neuronal population in monkey inferior temporal cortex. *Journal of Neurophysiology*, 97, 4296-4309.
- Kivisaari, S., Tyler, L., Monsch, A. & Taylor, K. (2012). Medial perirhinal cortex disambiguates confusable objects. *Brain*, 135, 3757-3769.
- Kriegeskorte, N., Mur, M., Ruff, D., Kiani, R., Bodurka, J., Esteky, H., Tanaka, K. & Bandetti, P. (2008) Matching categorical object representations in inferior temporal cortex of man and monkey. *Neuron*, 60, 1126-1141.
- Kumaran, D., Melo, H. & Duzel, E. (2012). The emergence and representation of knowledge about social and nonsocial hierarchies, *Neuron*, 76, 653-666.
- Kumaran, D., Summerfield, J., Hassabis, D & Maguire, E. (2009). Tracking the emergence of conceptual knowledge during human decision making, *Neuron*, 63, 889-901.






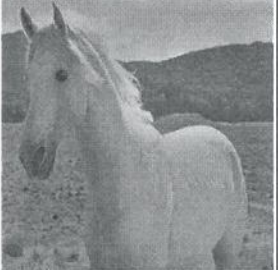
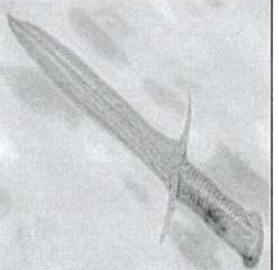



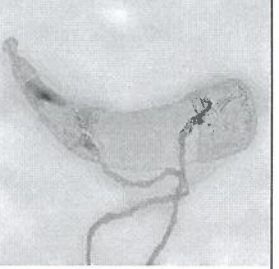
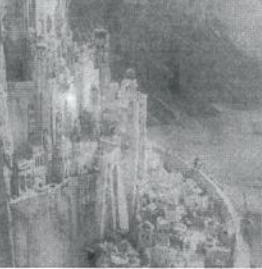


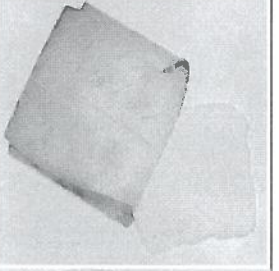





- Litman, L., Awipi, T. & Davachi (2009). Category-specificity in the human medial temporal lobe cortex. *Hippocampus*, 19, 308-319.
- Logothetis, N. (2008). What we can do and what we cannot do with fmri. *Nature*, 453, 869-878.
- Marques, J., Kober, T., Krueger, G., der Zwaag, W., de Moortele, P. & Gruetter, R. (2010). Mp2rage, a self bias-field corrected sequence for improved segmentation and t1-mapping at high field. *Neuroimage*, 49, 1271-1281.
- Martin, A., Wiggs, C., Ungeleider, L. & Haxby, J. (1996). Neural correlates of category-specific knowledge. *Neuron*, 379, 649-652.
- McClelland, J., McNaughton, B. & O'Reilly, R. (1995). Why there are complementary learning systems in the hippocampus and neocortex: Insights from the successes and failures of connectionist models of learning and memory. *Psychological Review*, 102, 419-457.
- Milivojevic, B. & Doeller, C. (2013). Mnemonic networks in the hippocampal formation: From spatial maps to temporal and conceptual codes. *Journal of Experimental Psychology*, 142, 1231-1241.
- Millikan, R. (1998). A common structure for concepts of individuals, stuffs, and real kinds: More mama, more milk, and more mouse. *Behavioral and Brain Sciences*, 9, 55-100.
- Mion, M., Patterson, K., Acosta-Cabronero, J., Pengas, G., Izquierdo-Garcia, D., Hong, Y., Fryer, T., Williams, G., Hodges, J. & Nestor, P. (2010). What the left and right anterior fusiform gyri tell us about semantic memory. *Brain*, 133, 3256-3268.
- Moore, C. & Price, C. (1999). A functional neuroimaging study of the variables that generate category-specific object processing differences. *Brain*, 122, 943-962.
- Moss, H., Rodd, J., Stamatakis, E., Bright, P. & Tyler, L. (2005). Anteromedial temporal cortex supports fine-grained differentiation among objects. *Cerebral Cortex*, 15, 616-627.

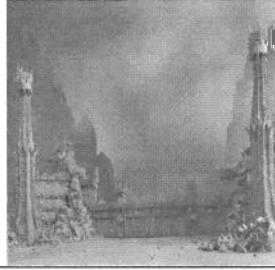
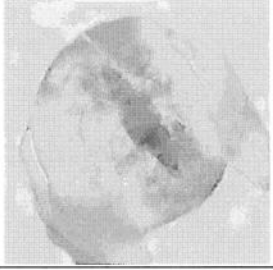
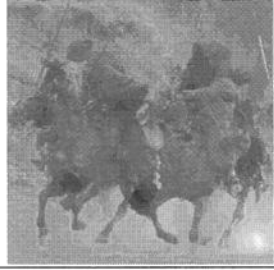
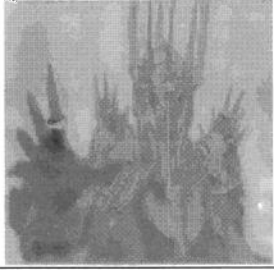
- Mummary, C., Patterson, K., Hodges, J. & Wise, R. (1996). Retrieving ‘tiger’ as an animal name or a word beginning with t: Differences in brain activation. *Proceedings of the Royal Society B: Biological Sciences*, 263, 989-995.
- O’Toole, A., Jiang, F., Abdi, H. & Haxby, J. (2005). Partially distributed representations of objects and faces in ventral temporal cortex. *Journal of Cognitive Neuroscience*, 17, 580–590.
- Op de Beeck, H., Brants, M., Baeck, A. & Wagemans, J. (2010). Distributed subordinate specificity for bodies, faces, and buildings in human ventral visual cortex. *Neuroimage*, 49, 3414–3425.
- Poser, B., Koopmans, P., Witzel, T. Wald, L. & Barth, M. (2010). *Neuroimage*, 51, 261-266.
- Putnam, H. (1973). Meaning and reference. *The Journal of Philosophy*, 70, 699-711.
- Reddy, L. & Kanwisher, N. (2007). Category selectivity in the ventral visual pathway confers robustness to clutter and diverted attention. *Current Biology*, 17, 2067–2072.
- Scoville, W. B. & Milner, B. (1957). Loss of recent memory after bilateral hippocampal Lesions. *Journal of Neurology, Neurosurgery and Psychiatry*, 20, 11–21.
- Shohamy, D. & Wagner, A. (2008). Integrating memories in the human brain: Hippocampal-midbrain encoding of overlapping event. *Neuron*, 60, 378-389.
- Simanova, I., Hagoort, P., Oostenveld, R. & van Gerven, M. (2014). Modality-independent decoding of semantic information from the human brain. *Cerebral Cortex*, 24, 426-434.
- Smith, S. & Nichols, T. (2009). Threshold-free cluster enhancement: addressing problems of smoothing, threshold dependence and localization in cluster inference. *Neuroimage*, 44, 83-98.
- Smith, S. (2002). Fast robust automated brain extraction. *Human Brain Mapping*, 17, 143-155.

- Spiridon, M. & Kanwisher, N. (2002). How distributed is visual category information in human occipito-temporal cortex? An fmri study. *Neuron*, 35, 1157–1165.
- Staresina, B. & Davachi, L. (2009). Mind the gap: Binding experiences across space and time in the human hippocampus. *Neuron*, 63, 267-267.
- Taylor, K, Moss, H., Stamatakis, E. & Tyler, L. (2006). Binding crossmodal object features in perirhinal cortex. *Proceedings of the National Academy of Sciences*, 103, 8239-8244.
- Taylor, K, Stamatakis, E. & Tyler, L. (2009). Crossmodal integration of object features: Voxel-based correlations in brain-damaged patients. *Brain*, 132, 671-683.
- Tzourio-Mazoyer, N., Landeau, B, Papathanassiou, D., Crivello, F., Etard, O., Delcroix, N., Mazoyer, B. & Joliot, M. (2002). Automated anatomical labeling of activations in spm using a macroscopic anatomical parcellation of the mni mri single-subject brain. *Neuroimage*, 15, 273-89.
- Verhagen, L., Dijkerman, H. C., Grol, M. J. & Toni, I. (2008). Perceptuo-motor interactions during prehension movements. *Journal of Neuroscience*, 28, 4726-35.
- Viskontas, I., Quian Quiroga, R. & Fried, I. (2009). Human medial temporal lobe neurons respond preferentially to personally relevant images. *Proceedings of the National Academy of Sciences*, 106, 21329-21334.
- Warrington, E. & Shallice, T. (1984). Category specific semantic impairments. *Brain*, 107, 829-854.
- Willenbockel, V., Sadr, J., Fiset, D., Horne, G., Gosselin, F. & Tanaka, J. (2010). Controlling low-level image properties: The shine toolbox. *Behavior Research Methods*, 42, 671-684.
- Winkler, A., Ridgway G., Webster M., Smith S. & Nichols T. (2014). Permutation inference for the general linear model. *Neuroimage*, 92, 381-397
- Zhan, H., Tian, J., Liu, J, Li, J. & Lee, K. (2009). Intrinsically organized networks for face perception during the resting state. *Neuroscience Letters*, 454, 1-5.

Supplementary material

THE LORD OF THE RINGS

| Faces | Animals | Objects | Scenes |
|---|---|--|---|
|  |  |  |  |
|  |  |  |  |
|  |  |  |  |
|  |  |  |  |
|  |  |  |  |



Harry Potter

| Faces | Animals | Objects | Scenes |
|-------|---------|---------|--------|
| | | | |
| | | | |
| | | | |
| | | | |

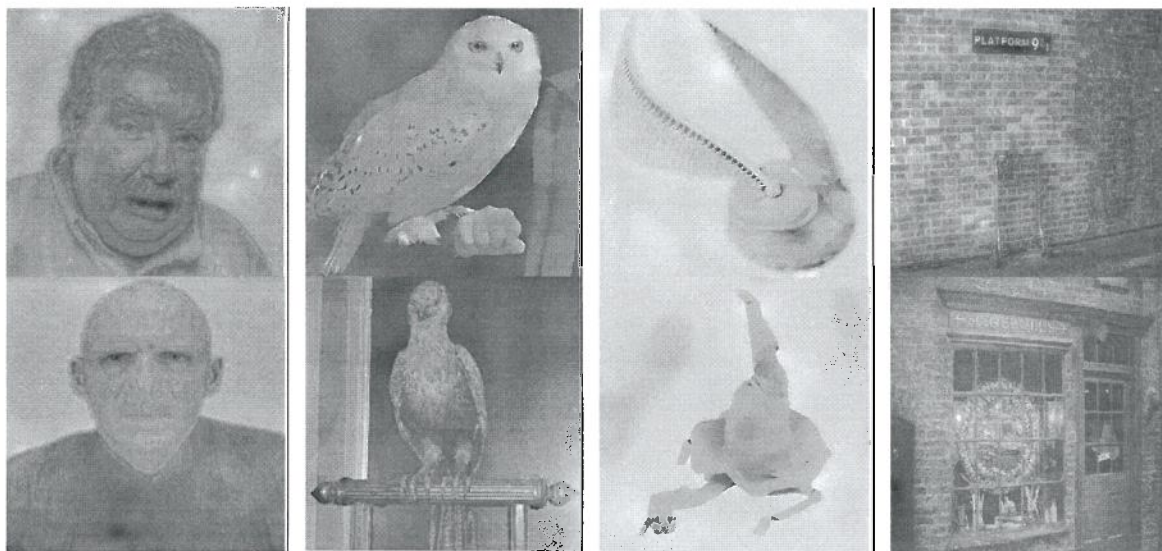


Fig. S1 Experimental stimuli after low-level normalization with the SHINE toolbox.



Fig. S2 Arena task. Participants were instructed to arrange the objects according to how related they think they are.

Table S1. Summary of regions that show a significant BOLD response for *scenes > faces, animals, objects*.

| Region (peak) | MNI coordinates | | | z value |
|---------------------------------|-----------------|------|-----|---------|
| | X | Y | Z | |
| <i>R Cerebellum</i> | 26 | -40 | -22 | 5.47 |
| <i>L Fusiform gyrus</i> | -32 | -46 | -14 | 5.67 |
| <i>R Calcarine sulcus</i> | 20 | -62 | 14 | 5.27 |
| <i>R Middle occipital gyrus</i> | 46 | -82 | 26 | 4.91 |
| <i>L Middle occipital gyrus</i> | -38 | -90 | 24 | 4.99 |
| <i>L Lingual gyrus</i> | -20 | -100 | -18 | 3.69 |

MNI coordinated and z statistics are shown (from biggest to smallest cluster) for all regions with significantly higher activity ($p < .05$, cluster-corrected; cluster size > 10 voxels). L, left; R, right.

Table S2. Summary of regions that show a significant BOLD response for *objects > faces, animals, scenes*.

| Region (peak) | MNI coordinates | | | z value |
|--|-----------------|-----|-----|---------|
| | X | Y | Z | |
| <i>L Lingual gyrus</i> | 0 | -82 | 4 | 5.28 |
| <i>L Precentral gyrus</i> | -56 | 6 | 42 | 3.91 |
| <i>R Inferior frontal gyrus, triangular part</i> | 54 | 34 | 14 | 3.41 |
| <i>R Inferior frontal gyrus, orbital part</i> | 42 | 24 | -14 | 3.67 |
| <i>L Inferior frontal gyrus, orbital part</i> | -42 | 24 | -8 | 3.41 |
| <i>L Middle frontal gyrus</i> | -36 | 56 | 20 | 2.88 |
| <i>R Supplementary motor area</i> | 2 | 10 | 54 | 3.42 |
| <i>L Supplementary motor area</i> | -4 | 10 | 72 | 3.43 |
| <i>R Cerebellum</i> | 38 | -64 | -60 | 2.38 |
| <i>L Caudate nucleus</i> | -8 | 10 | 0 | 2.11 |

MNI coordinated and z statistics are shown (from biggest to smallest cluster) for all regions with significantly higher activity ($p < .05$, cluster-corrected; cluster size > 10 voxels). L, left; R, right.

Table S3. Summary of regions that show a significant BOLD response for *animals > faces, objects, scenes*.

| <i>Region (peak)</i> | <i>MNI coordinates</i> | | | <i>z value</i> |
|---------------------------------|------------------------|----------|----------|----------------|
| | <i>X</i> | <i>Y</i> | <i>Z</i> | |
| <i>R Middle occipital gyrus</i> | 54 | -76 | -2 | 4.44 |

MNI coordinated and z statistics are shown (from biggest to smallest cluster) for all regions with significantly higher activity ($p < .05$, cluster-corrected; cluster size > 10 voxels). L, left; R, right.

Table S4. Summary of regions that show a significant BOLD response for *faces > animals, objects, scenes*.

| <i>Region (peak)</i> | <i>MNI coordinates</i> | | | <i>z value</i> |
|---|------------------------|----------|----------|----------------|
| | <i>X</i> | <i>Y</i> | <i>Z</i> | |
| <i>R Superior frontal gyrus, medial</i> | 6 | 56 | 28 | 4.27 |
| <i>L Precuneus</i> | 2 | -62 | 30 | 3.87 |

MNI coordinated and z statistics are shown (from biggest to smallest cluster) for all regions with significantly higher activity ($p < .05$, cluster-corrected; cluster size > 10 voxels). L, left; R, right.

Table S5. Summary of regions that show a significant BOLD response for *faces, animals > objects, scenes*.

| <i>Region (peak)</i> | <i>MNI coordinates</i> | | | <i>z value</i> |
|---|------------------------|----------|----------|----------------|
| | <i>X</i> | <i>Y</i> | <i>Z</i> | |
| <i>L Middle frontal gyrus, orbital part</i> | -2 | 64 | -2 | 4.2 |
| <i>L Superior frontal gyrus, medial</i> | -2 | 56 | 30 | 4.02 |
| <i>L Precuneus</i> | 0 | -62 | 26 | 4.39 |
| <i>R Middle temporal gyrus</i> | 58 | -68 | 16 | 3.92 |

MNI coordinated and z statistics are shown (from biggest to smallest cluster) for all regions with significantly higher activity ($p < .05$, cluster-corrected; cluster size > 10 voxels). L, left; R, right.

Table S6. Summary of regions that show a significant RSA effect for *animals*.

| Region (peak) | MNI coordinates | | | z value |
|---|-----------------|------|----|---------|
| | X | Y | Z | |
| <i>R Inferior occipital gyrus</i> | 44 | -82 | -6 | 3.93 |
| <i>L Middle occipital gyrus</i> | -42 | -90 | 12 | 3.38 |
| <i>L Calcarine fissure and surrounding cortex</i> | 8 | -102 | 12 | 3.11 |
| <i>R Calcarine sulcus</i> | 8 | -74 | 8 | 2.96 |
| <i>R Precuneus</i> | 4 | -62 | 60 | 3.33 |

MNI coordinated and z statistics are shown (from biggest to smallest cluster) for all regions with significantly higher similarity for within than across categories ($p < .05$, cluster-corrected; cluster size > 10 voxels). L, left; R, right.

Table S7. Summary of regions that show a significant RSA effect for *scenes*.

| Region (peak) | MNI coordinates | | | z value |
|---|-----------------|-----|-----|---------|
| | X | Y | Z | |
| <i>L Fusiform gyrus</i> | -40 | -48 | -18 | 4.2 |
| <i>L Superior frontal gyrus, dorsolateral</i> | -20 | 2 | 50 | 4.02 |
| <i>L Postcentral gyrus</i> | -44 | -40 | 66 | 4.39 |

MNI coordinated and z statistics are shown (from biggest to smallest cluster) for all regions with significantly higher similarity for within than across categories ($p < .05$, cluster-corrected; cluster size > 10 voxels). L, left; R, right.

Table S8. Summary of regions that show a significant RSA effect for *objects*.

| Region (peak) | MNI coordinates | | | z value |
|--|-----------------|-----|-----|---------|
| | X | Y | Z | |
| <i>L Inferior occipital gyrus</i> | -48 | -76 | -6 | 4.28 |
| <i>R Superior frontal gyrus, dorsolateral</i> | 14 | 12 | 46 | 3.53 |
| <i>L Inferior frontal gyrus, opercular part</i> | -50 | 8 | 24 | 3.26 |
| <i>L Inferior parietal, excluding supramarginal and angular gyri</i> | -44 | -44 | 38 | 3.19 |
| <i>L Cerebellum</i> | -14 | -76 | -54 | 2.84 |
| <i>R Insula</i> | 42 | 18 | -4 | 2.97 |
| <i>R Inferior frontal gyrus, triangular part</i> | 46 | 28 | 22 | 2.82 |
| <i>R Anterior cingulate and paracingulate gyri</i> | 14 | 42 | 24 | 2.49 |
| <i>R Cerebellum</i> | 20 | -58 | -44 | 2.44 |
| <i>R Superior frontal gyrus, dorsolateral</i> | 20 | 0 | 74 | 2.59 |

MNI coordinated and z statistics are shown (from biggest to smallest cluster) for all regions with significantly higher similarity for within than across categories ($p < .05$, cluster-corrected; cluster size > 10 voxels). L, left; R, right.

Table S9. Summary of regions that show a significant RSA effect for *faces*.

| Region (peak) | MNI coordinates | | | z value |
|--|-----------------|-----|-----|---------|
| | X | Y | Z | |
| <i>R Calcarine sulcus</i> | 20 | -74 | 16 | 4 |
| <i>R Precuneus</i> | 4 | -54 | 54 | 3.79 |
| <i>R Lingual gyrus</i> | 16 | -98 | -12 | 3.15 |
| <i>L Inferior parietal, excluding supramarginal and angular gyri</i> | -28 | -36 | 34 | 2.74 |
| <i>R Cerebellum</i> | 14 | -82 | -20 | 2.53 |
| <i>R Middle temporal gyrus</i> | 42 | -52 | 10 | 2.78 |
| <i>R Inferior parietal, excluding supramarginal and angular gyri</i> | 36 | -46 | 34 | 2.78 |

MNI coordinated and z statistics are shown (from biggest to smallest cluster) for all regions with significantly higher similarity for within than across categories ($p < .05$, cluster-corrected; cluster size > 10 voxels). L, left; R, right.

Table S10. Summary of regions that show a significant RSA effect for *animacy*.

| Region (peak) | MNI coordinates | | | z value |
|--|-----------------|-----|-----|---------|
| | X | Y | Z | |
| <i>R Calcarine sulcus</i> | 18 | -66 | 6 | 3.72 |
| <i>L Median cingulate and paracingulate gyri</i> | -2 | -2 | 32 | 2.97 |
| <i>R Middle frontal gyrus</i> | 40 | 34 | 46 | 3.28 |
| <i>L Caudate nucleus</i> | -14 | 16 | 18 | 2.74 |
| - | -16 | -34 | 24 | 2.83 |
| <i>R Parahippocampal gyrus</i> | 20 | -38 | -12 | 2.82 |
| <i>L Superior parietal gyrus</i> | -28 | -50 | 58 | 2.49 |
| <i>L Thalamus</i> | -14 | -26 | 12 | 2.74 |
| <i>L Superior frontal gyrus, dorsolateral</i> | -18 | 40 | 54 | 3.2 |
| <i>L Lingual gyrus</i> | -20 | -76 | -10 | 2.51 |
| - | 32 | -44 | 16 | 2.28 |

MNI coordinated and z statistics are shown (from biggest to smallest cluster) for all regions with significantly higher similarity for within than across categories ($p < .05$, cluster-corrected; cluster size > 10 voxels). L, left; R, right.

Table S11. Summary of regions that show a significant BOLD response for *HP > LotR*.

| Region (peak) | MNI coordinates | | | z value |
|---|-----------------|-----|-----|---------|
| | X | Y | Z | |
| <i>L Parahippocampal gyrus</i> | -26 | -14 | -32 | -26 |
| <i>L Inferior frontal gyrus, orbital part</i> | -42 | 32 | -20 | -42 |
| <i>L Calcarine fissure and surrounding cortex</i> | 0 | -86 | -18 | 0 |
| <i>R Caudate nucleus</i> | 16 | -22 | 20 | 16 |
| <i>R Fusiform gyrus</i> | 34 | -28 | -30 | 34 |
| <i>R Parahippocampal gyrus</i> | 22 | -14 | -36 | 22 |
| <i>R Precentral gyrus</i> | 34 | -2 | 28 | 34 |
| <i>L Parahippocampal gyrus</i> | -26 | -14 | -32 | -26 |

MNI coordinated and z statistics are shown (from biggest to smallest cluster) for all regions with significantly higher activity ($p < .05$, cluster-corrected; cluster size > 10 voxels). L, left; R, right.

Table S12. Summary of regions that show a significant BOLD response for *LotR* > *HP*.

| <i>Region (peak)</i> | <i>MNI coordinates</i> | | | <i>z value</i> |
|---|------------------------|----------|----------|----------------|
| | <i>X</i> | <i>Y</i> | <i>Z</i> | |
| <i>R Insula</i> | 30 | 16 | -18 | 5.21 |
| <i>L Calcarine fissure and surrounding cortex</i> | -10 | -106 | 4 | 4.15 |
| <i>L Inferior temporal gyrus</i> | 64 | -28 | -28 | 3.11 |
| <i>R Precentral gyrus</i> | 62 | 6 | 24 | 2.52 |

MNI coordinated and z statistics are shown (from biggest to smallest cluster) for all regions with significantly higher activity ($p < .05$, cluster-corrected; cluster size > 10 voxels). L, left; R, right.